Case Studies in Thermal Engineering 18 (2020) 100608

Contents lists available at ScienceDirect

Case Studies in Thermal Engineering

journal homepage: http://www.elsevier.com/locate/csite

Continuous walking-beam furnace 3D zonal model and direct thermal-box barrier based temperature measurement

Michal Švantner *, Josef Študent, Zdeněk Veselý

University of West Bohemia, Univerzitní 8, 301 00, Plzeň, Czech Republic

ARTICLE INFO

Keywords:
Furnace
Walking-beam furnace
Radiation heat transfer
Numerical model
Hottel zonal method
Thermal box-barrier
Temperature measurement

ABSTRACT

Numerical simulation of industrial reheating furnaces belongs to important procedures for an optimization of their design and processing parameters. A 3D numerical model of a continuous gas burners heated walking-beam furnace is introduced in this paper. The main benefit of the model is a compromise between its complexity and computing speed. The model connects numerical procedures and empirical knowledge. It is based on a Hottel zonal method and a compartment based solution of heat transfer process in solids. It allows specifying charge, heating system and furnace parameters. The solution includes convective and radiative heat transfer in the furnace including a participation of a semi-transparent gaseous furnace atmosphere. A direct measurement of charge temperature course in a walking-beam furnace using thermocouples and thermal box-barrier are introduced. Comparisons of the measurement results with results of numerical simulations are presented. Connection between direct measurement in the furnace and the numerical simulation parameters is discussed. A good agreement between the theoretical and measured data shows, that the model includes the most important physical process.

1. Introduction

Heat treatment of products or their heating before subsequent technological operations is a commonly used technological operation in many kinds of industry. Periodical, continuous or carrousel type furnaces [1] are often used for example in steel or ceramics processing industry as a part of production lines. The processing temperatures in such furnaces significantly exceed 1000 °C [2] in many cases and the industrial continuous furnaces operators are very large energy consumers. An optimization of an operation of the furnaces can therefore bring charge heating process technological improvements as well as significant fuel consumption savings, financial savings and a reduction of a production of environmentally harmful substances.

The optimization of the furnace operation is mostly based on a numerical modeling of thermal processes during charge heating [3]. Complex numerical models are developed for a detailed description and understanding of the processes inside the furnace. These models are mostly based on continuum fluid mechanics methods and are focused on maximum mathematical description of all the important processes. This approach is important for an understanding of the processes and their interaction. The models are mostly very extensive, have huge demands on computing resources and a calculation takes a long time. Thus, this approach is not too suitable for an on-line optimization or processing parameters correction. The complex walking-beam continuous furnace 3D numerical modelling is presented for example in Ref. [4] or [5]. A 3D unsteady numerical simulation of a reheating furnace was performed to

* Corresponding author. University of West Bohemia - New Technologies Research Centre, Univerzitní 8, 306 14, Plzeň, Czech Republic.
E-mail addresses: msvantne@ntc.zcu.cz (M. Švantner), studentj@ntc.zcu.cz (J. Študent), zvesely@ntc.zcu.cz (Z. Veselý).

https://doi.org/10.1016/j.csite.2020.100608
Received 18 November 2019; Received in revised form 23 January 2020; Accepted 17 February 2020
Available online 18 February 2020

List of symbols

$a_{k[j]}$	heat transfer coefficient to j-th surface of a zone by convection (W $m^{-2}K^{-1}$)
$c_{sp[i]}$	specific heat of combustion product in i-th zone (J $kg^{-1}K^{-1}$)
i	zone number index
j	surface number index
k	surface number index
$m_{ko[i]}$	mass flow of combustion products to chimney (kg s^{-1})
$m_{sh[i]}$	mass flow of combustion products from burners (kg s^{-1})
$m_{sp[i]}$	mass flow of combustion products between zones (kg s^{-1})
m_{vs}	charge mass (kg) - a shift given by walking beam mechanism
$M_{sp[i]}$	mass of combustion products in the *i*-th zone (kg)
N	a number of isothermal surfaces in a zone
$q_{[j]}$	specific radiation heat flow outgoing from *j*-th surface (W m^{-2})
$q_{k[j]}$	heat flow into *j*-th surface of a zone by convection (W)
$q_{ko[i]}$	heat flow of combustion products into a chimney (W)
$q_{sh[i]}$	heat flow from burners (W)
$q_{sp[i]}$	heat flow of combustion products between zones (W)
$q_{vs[i]}$	heat transferred by charge (J) - a shift given by walking beam mechanism
$q_{vz[i]}$	heat flow of combustion air (W)
$q_{zt[i]}$	a sum of all additional dissipation heat fluxes (W)
$Q_{sp[i]}$	heat content of combustion products in the *i*-th zone (J)
$S_{[j]}$	area of the *j*-th surface of a zone (m^2)
t	time (s)
$t_{[j]}$	temperature of the *j*-th surface of a zone (°C)
$T_{[j]}$	absolute temperature of the *j*-th surface of a zone (K)
$tz_{[i]}$	combustion products temperature in the *i*-th zone (°C)
Tz	combustion products absolute temperature in a zone (K)
$\alpha_{[k,j]}$	absorption of an environment between the *k*-th and *j*-th surface
$\delta_{[k,j]}$	Kronecker symbol (−)
$\varepsilon_{[j]}$	relative emissivity of the *j*-th surface
$\phi_{[k,j]}$	angular coefficient of radiation from the *k*-th surface to the *j*-th surface
σ	Stefan-Boltzmann constant (W m^{-2} K^{-4})
$\tau_{[j,k]}$	transparency of an environment between the *k*-th and *j*-th surface

obtain the optimal slab residence time for a walking beam type reheating furnace in Ref. [6]. A complex model of three-dimensional simulation of walking beam furnace was developed in Ref. [7], where the modeling results were compared with measured results. Two 3D heat transfer models based on finite volumes method for predicting the transient heat transfer characteristics of slabs in a walking beam reheating furnace were introduced in Ref. [8].

Simplified numerical models are developed for furnace operation process parameters optimization. These models are mostly based on various simplifications, for example, geometric simplifications or a reduction of processes solved. A lot of empirical knowledge are mostly required for these models, which should be determined using the complex numerical models or by direct measurements on real furnaces. However, these models are fast enough and can be used for an on-line optimization of a furnace operation, often as a part of a furnace control system. Such a model developed for a continuous furnace optimal heating control system is introduced for example in Ref. [9].

Rigorous numerical models are mostly too extensive and time consuming, on the other hand, simplified models are mostly adapted to a particular furnace and do not offer required variability and parameters adaptation possibilities. Thus, compromise numerical procedures are developed, which offer an acceptable variability, solution accuracy and computing speed. These solutions could be based on computational fluid dynamics [10], however, one of the favorite approaches are zonal models. Adaptations of zonal models for furnaces numerical modelling is presented, for example, in Refs. [11,12] or [13]. These models are based on dividing of the furnace volume to several zones. The combined radiative and convection heat transfer problem in individual zones and a heat transfer exchange between zones are solved separately. A hybrid zone-CFD model, which combines some advantages of the zone method and Computational Fluid Dynamics, is introduced in Ref. [14].

A numerical modelling of industrial furnaces should be supported by a direct measurement, which should be used for a numerical model design, parameters improvement, and results verification. The temperature measurement of the furnace or charge can be performed using both contact and non-contact methods. Temperature measurement in continuous furnaces are described for example in Refs. [2,15]. Basic measurement equipment is mostly a part of industrial furnaces and consists of on-furnace installed thermocouples and pyrometers. Such a measurement system gives permanent information about furnace zones temperature (thermocouples) and charge temperature at given positions (pyrometers). Three different temperature measurement methods were compared and validated

by computational fluid dynamics in Ref. [16]. More sophisticated charge temperature measurement during its movement throughout the furnace can be carried out using a special thermal box-barrier device, as described in Ref. [17]. A similar thermal protection device was also used in Ref. [18]. This measurement technique gives the best information of a charge temperature progress. However, it is far too complicated, and not applicable for a permanent charge temperature monitoring.

Numerical solutions of the processes in a walking-beam furnace presented in publications [5–8] were based on discretization and a full CFD analysis. These models included most of the relevant processes (turbulent flow, combustion, radiation etc.), and were solved using a commercial computational software. However, these models used a huge number of elements and a computation so took a very long time (1.2 mil. elements and 34 h reported in Ref. [6], 11.4 mil. cells reported in Ref. [7]). These models are therefore not suitable for an investigation of an influence of different parameters of heating characteristics or for a design of a furnace and/or a heating process. In contrast, a cost-effective zone model was presented in Ref. [11]. In the research presented in Ref. [11], a conservation of energy for each zone was computed based on directed flux areas (DFA), the wall emissivity was assumed independent on temperature and an empirical correlation was used for a calculation of convective coefficients. Heat flux and temperature in billets were solved in 3D by their dividing into uniform elements. Numerical computation results were compared with thermocouple based measurement; however, a measurement procedure was not described in detail. A contribution of a convection and an influence of furnace wall emissivity was analyzed using the described model.

A zonal model based 3D solution is adapted in this work for a walking beam type furnace numerical modelling. In contrast to Ref. [11], the approach in this work is based on a computation of radiation view factors and mean geometric lengths, which is performed by dividing of surfaces to small elements. Analytical procedures of a computation of the radiation view factors and mean geometric lengths is then combined with a numerical solution of a heat transfer problem. The solution includes radiation and convection problem inside the furnace, participating of a semi-transparent gaseous media inside the furnace, charge movement and heat transfer in charge and furnace parts (furnace walls for example). A conductive heat transfer in billets is made using a division to compartments. It provides a less detailed spatial analysis than division to element used in Ref. [11]; however, much fewer elements are needed. The used approach can bring improvements in a computing time. It also allows a development of a good adaptable model, which can fully be configured parametrically. Results of numerical analyses are verified by a direct measurement of a billet temperature during its passage through a furnace. The measurement procedure is described and an influence of a correct setting of experimentally determined temperature in a zone of the furnace is demonstrated by the comparison of the experimental and numerical results.

2. Walking beam furnace processes overview

Walking beam furnace [5,19,20] is a continuous type furnace. A charge is often in a shape of beams, rods, tubes or sheets, which move through the furnace from one end to the other. The movement of the charge provides a mechanism, which shifts or transfers individual pieces of the charge to a next position in defined intervals using fixed and moving supports. The movement is performed by a hydraulic system, which is often used also for other moving parts of the furnace (e.g. input and output gates). A specific feature of the walking beam furnaces is that individual charge pieces are separated [11,21]. Charge pieces in a pusher type furnace, for example, are often in a direct contact and it is sometimes possible to simplify a series of charge pieces as a one continuous part. Compared to that, each piece of the charge in walking beam furnaces has to be assumed individually and geometrical definitions for a heat transfer computational model, especially for a radiation heat transfer model, are then more complicated.

The main parts of walking beam furnaces are outer casing (a steel construction), movement mechanism, hydraulic system, heating system, combustion products outlet system, refractory brickwork and a moving parts lubrication system. Some components inside the furnace are cooled, thus, a water cooling system is also a part of the furnace. Gas burners based heating system is mostly used for steel charge heating, where the maximum service temperature can reach up to 1300 °C. The furnaces can be several tens meters long and they are often divided into several zones.

The charge heating process is mostly defined by a heating curve, which prescribes a required temperature of the charge in each position and time in the furnace. The most of furnace control systems correlate the charge temperature to a furnace temperature, which is defined for each zone in the furnace. The furnace temperature is, in the simplest case, represented by temperature measured by furnace thermocouples located in the zones. A relationship between the charge temperature during its passage through the furnace and the furnace zone temperatures is mostly defined by a heating function. The heating function can be obtained by a numerical model accompanied by an experimental calibration. The control system of the furnace then uses information about the charge (material, size, time in furnace etc.), furnace temperature provided by the thermocouples and the heating function for an optimization of a heating process. The optimization is mostly performed in such a way that the estimated charge temperature approaches the temperature specified by the heating curve.

3. Heating proces numerical model

A gas-burner type continuous reheating furnace operation is a very complex process, which includes convection, conduction and radiation heat transfer, combustion products turbulent flow, chemical reactions (combustion) and interactions with the furnace surroundings [5]. The process is non-linear and most of material properties entering the process are dependent on temperature. The process is unsteady and should be solved as three-dimensional because of radiation geometrical dependencies. The main parts of the process are:

- Heat input into the furnace due to burners. Flames and burning products distribute the heat inside the furnace space by radiation and convection.
- Heat exchange inside the furnace. It includes an exchange between burning products and furnace walls, furnace inner components and charge; and radiation heat transfer between surfaces inside the furnace (charge, walls etc.). Furnace atmosphere (combustion products) limited transmissivity has to be taken into account. Specific spectral range of the combustion products were not assumed in this model.
- Internal heat transfer processes. The internal heat transfer includes heating up (or cooling) and conduction in charge, furnace walls and other bodies in the furnace. Temperature dependence of thermal properties of materials is taken into account.
- Heat losses. A part of the heat removed by combustion products through a chimney, by cooling of the furnace by surroundings or by cooling water in cooled parts of the furnace.

The radiation heat transfer becomes dominant at high temperatures, therefore, a special attention should be given to this process [12,20]. The radiation heat flux is defined by the radiating surfaces temperatures (a proportionality to the 4th power difference), their geometrical configuration and their optical properties (emissivity). The geometrical configuration is defined by a radiation view factor, which describes a mutual visibility of the radiating surfaces. The emissivity [15] of the surfaces is the radiometric dimensionless quantity, which describes their thermal radiation properties. Combustion products between surfaces can influence the thermal process by absorption and emission of a radiation heat. Combustion products in gas-burner furnaces are mostly partially transparent. Their emissivity, absorptivity and transmissivity are dependent on their chemical composition, chemical reactions, wavelengths, thermodynamic state of the gas (pressure, temperature) and a thickness of their layer (a characteristic length). Burning gas combustion products typically emit and absorb radiation on specific wavelengths only. A more detailed description of radiation heat transfer can be found also for example in book [22].

The model developed and applied in this work was based on a connection of numerical procedures and empirical knowledge. It allows a definition of following variables:

- Charge-beams parameters: dimensions, material properties in dependence on temperature, surface properties and discretization.
- Furnace parameters: number of beams in the furnace, initial temperature of beams, movement frequency (performance of the furnace), surroundings temperature and convection coefficient, combustion air temperature (including recuperation), combustion air humidity, burning gas parameters (properties, temperature, humidity), overpressure in the furnace and number of zones.
- Computational time step length and final time at which the process is assumed stable.
- Individual zones parameters: dimensions of the zone, furnace hearth position, beams step length, number of beams in the zone, number and thickness of layers forming walls, material properties of the walls, discretization parameters of the walls, number of burners, type of burners (high-speed, whirling, radiant), definition of cooled parts, definition of water ducts, definition of heat loses due cooled rollers, definition of furnace openings (dimensions and relative time at which are opened).

A geometry of a walking-beam furnace is divided into a several computational zones based on geometry of the furnace and required heating-curve gradient. Combustion products temperature distribution is assumed constant in one zone. A mutual radiation heat transfer between combustion products, furnace walls and individual beams (charge) is solved according to the Hottel zonal method in each zone and in each time step. Emissivity and/or absorptivity of surfaces and combustion products as well as other material properties are assumed temperature dependent. The properties are updated in each time step according to a current temperature. A classical Newton's law is used for a convective heat transfer definition. The convective heat transfer coefficients are estimated based on empirical knowledge end experimental calibrations according to types of burners in each zone. Such simplification is sufficient considering that radiation plays a crucial role. Thus, combustion products flow does not need to be calculated numerically. The individual beams as well as furnace walls are divided into compartments. A conduction heat transfer is assumed between the compartments.

The results of heat transfer process are included into heat and mass exchange computation for each zone. Energy balance between entering (burners, combustion products, heat flux, moving charge beams) and leaving (combustion products, moving charge beams, heat flux, heat losses) heat/mass flow is solved in each time step. Interaction between individual zones is limited to a transfer of the combustion products and beams. Radiation between zones is not assumed. A resultant differential equation system is solved by a Merson's modification of Runge-Kutta 4th order method, which allows an automatic change of a time step length. A complete solution of the model including all computational procedures was implemented in an own software developed within the research. The principal result is a simulation of heating of the beams during their passage throughout the furnace. Additionally, other thermal information are obtained by the computation, for example, combustion products temperature, required amount of cooling water, heat and mass fluxes in the furnace etc.

A generally required result correspond to a steady state. However, the introduced simulation model is transient and a time to process steadiness is one of the determined parameters. This approach is more flexible compared to a standard steady-state solving procedure.

3.1. Energy balance in zones

Schematic representation of furnace dividing to zones including heat and mass fluxes between the zones is in Fig. 1. As follows from the figure, the energy balance of combustion products in a zone is

$$q_{vs[i-1]} - q_{vs[i]} - q_{zt[i]} + q_{sh[i]} + q_{sp[i+1]} - q_{sp[i]} - q_{ko[i]} + q_{vz[i]} = \frac{d\,Q_{sp[i]}}{d\,t} \tag{1}$$

where $Q_{sp[i]}$ is heat content of combustion products in the zone, $q_{vs[i]}$ is heat transferred by billets, $q_{zt[i]}$ is sum of all additional dissipation heat fluxes, $q_{sh[i]}$ is heat flow from burners, $q_{sp[i]}$ heat flow of combustion products between zones, $q_{ko[i]}$ is heat flow of combustion products into a chimney and $q_{vz[i]}$ is heat flow of combustion air. As a time variation of mass $M_{sp[i]}$ and specific heat $c_{sp[i]}$ of combustion products is negligible, it is possible to state eq. (1) to the form:

$$q_{vs[i-1]} - q_{vs[i]} - q_{zt[i]} + q_{sh[i]} + q_{sp[i+1]} - q_{sp[i]} - q_{ko[i]} + q_{vz[i]} = M_{sp[i]} \;.\; c_{sp[i]} \;.\frac{dtz_{[i]}}{dt} \tag{2}$$

where $tz_{[i]}$ is combustion products temperature in the zone, $c_{sp[i]}$ is specific heat of combustion product, $M_{sp[i]}$ is mass of combustion products.

The heat, which is transferred by the billets ($q_{vs[i]}$ and $q_{vs[i-1]}$), is realized every time a walking mechanism of the furnace sifts the billets. It is determined as the sum of heats in individual compartments, which is defined by their temperature, mass and specific heat. The dissipation heat flux in the individual zones $q_{zt[i]}$ is a sum of all additional outgoing heat fluxes. It includes losses due to front and rare walls of the furnace and due to a cooled steel frame of the walking beam mechanism. It was computed iteratively as a passage of heat through a wall. Further, it includes heat losses due to a radiation through technological openings and due to a radiation to water channels of the furnace mechanism. It was computed by Stefan-Boltzmann constant, area of the openings, coefficient of shielding and combustion products temperature 4th power. Heat flux from burners $q_{sh[i]}$ is computed accordingly to the requirement to maintain the defined/prescribed temperature in a heated zone (see below). The heat flux by combustion products flow between zones ($q_{sp[i]}$, $q_{sp[i+1]}$) is given by temperature, mass and specific heat of the combustion products. The same quantities define heat flow of combustion products into a chimney $q_{ko[i]}$. Finally, the heat flow of combustion air $q_{vz[i]}$ is given by its temperature, mass and specific heat.

The temperature is set as the control parameter if there is a burner in the zone (heated/controlled zone). In this case, the temperature is maintained at a required value by an adjustment of burners heat flux into the zone and the term $\frac{dtz_{[i]}}{dt}$ in eq. (2) is equal to zero. It makes possible to determine the required heat flux from the burners in the zone at each time step, which is necessary to maintain the required temperature in this zone:

$$q_{sh[i]} = -\,q_{vs[i-1]} + q_{vs[i]} + q_{zt[i]} - q_{sp[i+1]} + q_{sp[i]} + q_{ko[i]} - q_{vz[i]} \tag{3}$$

On the other hand, combustion products temperature in a zone without burners (non-heated/uncontrolled zone) is defined by solving of the equation

$$\frac{dtz_{[i]}}{dt} = \frac{1}{M_{sp[i]} \cdot c_{sp[i]}} \left(-\,q_{vs[i-1]} + q_{vs[i]} - q_{zt[i]} - q_{sh[i]} + q_{sp[i+1]} - q_{sp[i]} - q_{ko[i]} + q_{vz[i]} \right) \tag{4}$$

Accordingly, the energy balance for a heated zone (with burners) is given by Eq. (2), which contains all incoming and outgoing heat fluxes. An unknown variable is a burners heat flux $q_{sh[i]}$, which maintains a prescribed temperature in the zone. The energy balance in a non-heated zone (without burners) is given by eq. (4), where a heat flux from burners is equal to zero ($q_{sh[i]} = 0$) and an unknown variable, which is a result of a solution, is a temperature in this zone. Based on the zonal model approach, the combustion products temperature is the same in one zone, regardless whether it is a heated or non-heated zone. The temperatures in the zones are defined by a temperature curve along a whole furnace length. However, temperature step changes at boundaries of the zones (a piecewise constant curve) bring problems in a solving of a radiation heat transfer between the zones. Thus, the temperature curve is adjusted by such a way that a zone temperature is defined for points representing a center of the zone and linearly interpolated between these points. This adjustment is however made for purposes of radiation heat transfer modelling only and the combustion products

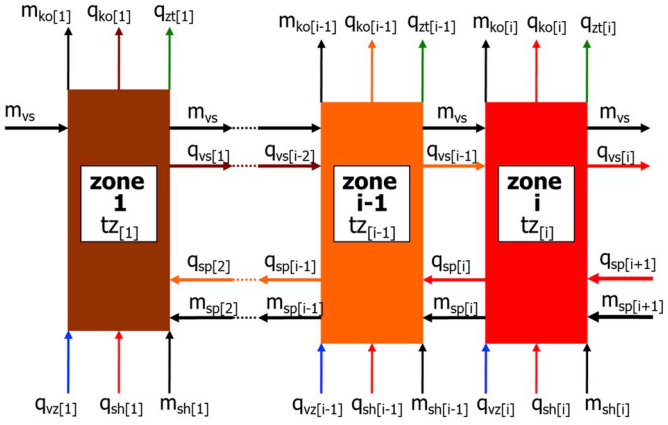

Fig. 1. Zones and schematic representation of heat and mass fluxes into and out of the zones.

temperature in a zone is still assumed homogeneous in accordance with the zonal model.

3.2. Heat transfer in a zone

Heat transfer between combustion products, furnace internal surfaces and beams surfaces inside a zone is the result of convection and radiation between each other. The radiation is solved in accordance with the Hottel zonal method [23,24]. The zone with *pzk* beams (*pzk* is the number of beams) consists of isothermal sub-zones. One sub-zone is an internal space of the zone, which is filled with a grey gas (combustion products). The space is surrounded by a set of *N* grey isothermal sub-zones, which represent internal surfaces (furnace walls and the beams) in the zone. It is necessary to point out, that one sub-zone can contain more surfaces. A geometrical representation of the 3D zonal model is in Fig. 2A. The picture shows one furnace zone, which contains one isothermal volume sub-zone (combustion products) and several isothermal surface sub-zones (furnace walls and billets surfaces).

Sub-zone $S_{[1]}$ represents furnace hearth, $S_{[2]}$ represents furnace ceiling and $S_{[3]}$ represents furnace side-walls. The beams have a rectangular cross-section. Each beam is divided to sub-zone $S_{[4]}(...S_{[3\cdot pkz+1]})$ representing its sides (front and back surfaces, which are against each other; side surfaces, which are against the furnace side-walls), a sub-zone $S_{[5]}(...S_{[3\cdot pkz+2]})$ representing its upper surface (against the furnace ceiling) and a sub-zone $S_{[6]}(...S_{[3\cdot pkz+3]})$ representing its bottom surface (against the furnace hearth).

The considered rectangular cross-section is a simplification, which makes possible a generic building of the model and which reduces a number of solved equations. Other shapes of a cross-section of the beams could be included, but it would increase a complexity of a solution of the radiation heat transfer. For example, a general polygonal cross-section could better approximate a very common circular cross-section. However, it would be more complicated for a determination of radiation geometrical relations as well as for a practical implementation. It would also bring longer computing times without a major effect on an accuracy of results. The approach used in this model was therefore based on a substitution of any cross-section shape with a corresponding rectangle.

Each sub-zone is divided to triangular elements and radiation view factors (RVFs) dϕ are solved for any pair of the elements. These partial RVFs are used for a numerical determination of integral RVFs $\phi_{[k,j]}$ (see eq. (5)), which defines radiation geometrical relations between entire sub-zones $S_{[k]}$ and $S_{[j]}$.

$$\phi_{[k,j]} = \frac{1}{S_{[k]}} \int_{S_{[k]}} \int_{S_{[j]}} \frac{\cos \phi_{[k]} . \cos \phi_{[j]}}{\pi r^2} \, d S_{[j]} \, . \, d S_{[k]} \tag{5}$$

The RVFs $\phi_{[k,j]}$ are computed for each two surfaces in every zone by a numerical integration, where $\phi_{[j,k]} = \frac{S_{[k]}}{S_{[j]}} . \phi_{[k,j]}$. The same procedure is used for a computation of a mean geometrical length $L_{[k,j]}$ for the each two surfaces

$$L_{[k,j]} = \frac{1}{S_{[k]} \, . \, \phi_{[k,j]}} \int_{S_{[j]}} \int_{S_{[k]}} \frac{\cos \phi_{[j]} . \cos \phi_{[i]}}{\pi r} \, d S_{[k]} \, . \, d S_{[j]} \tag{6}$$

where $L_{[j,k]} = L_{[k,j]}$. It is assumed that combustion products are ideally mixed in each zone (i.e. temperature and chemical composition are homogeneous). A transmissivity $\tau_{[j,k]}$ and an absorptivity $\alpha_{[j,k]}$ of the combustion products between each two surfaces (*j* and *k*) in a zone are then found in a material database based on the computed mean geometrical lengths $L_{[k,j]}$, chemical composition of the combustion products (CO_2, N_2 and H_2O) and their temperature. The radiation heat transfer is then solved for each pair of the considered sub-zones $S_{[1]} \ldots S_{[3\cdot pkz+3]}$ including combustion products between surfaces and multiple reflections from the furnace walls. The relationship between temperature of the isothermal surfaces and radiation heat flux into/from the surfaces can be then described by a system of *N* equations:

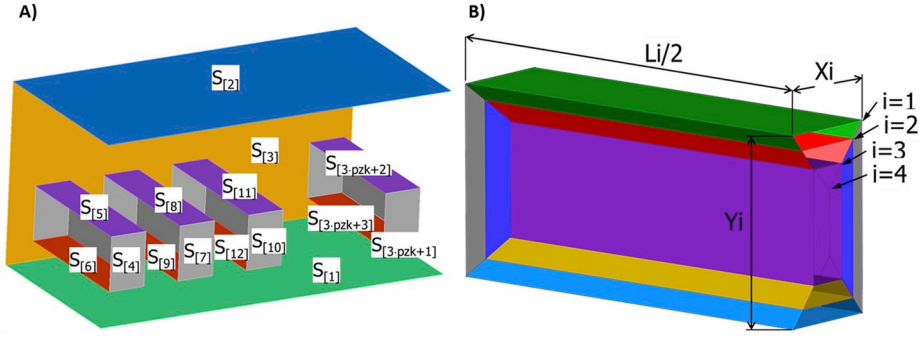

Fig. 2. Geometrical representation of the 3D model - a furnace zone (A) and a billet divided to compartments (B).

$$\sum_{j=1}^{N}\left(\frac{\delta_{[1,j]}}{\varepsilon_{[j]}}-\phi_{[1,j]}\frac{1-\varepsilon_{[j]}}{\varepsilon_{[j]}}\cdot\tau_{[j,1]}\right)\cdot q_{[j]}=\sum_{j=1}^{N}\left(\delta_{[1,j]}-\phi_{[1,j]}-\tau_{[j,1]}\right)\cdot\sigma\cdot T_{[j]}^{4}-\sum_{j=1}^{N}\phi_{[1,j]}\cdot\alpha_{[1,j]}\cdot\sigma\cdot Tz^{4}$$
$$\sum_{j=1}^{N}\left(\frac{\delta_{[N,j]}}{\varepsilon_{[j]}}-\phi_{[N,j]}\frac{1-\varepsilon_{[j]}}{\varepsilon_{[j]}}\cdot\tau_{[j,N]}\right)\cdot q_{[j]}=\sum_{j=1}^{N}\left(\delta_{[N,j]}-\phi_{[N,j]}-\tau_{[j,N]}\right)\cdot\sigma\cdot T_{[j]}^{4}-\sum_{j=1}^{N}\phi_{[N,j]}\cdot\alpha_{[N,j]}\cdot\sigma\cdot Tz^{4} \quad (7)$$

A solution of the equation system (7) provides a vector of radiation heat fluxes to individual surfaces in each zone.

Determination of geometrical relationships for radiation heat transfer according to Eqs. (5) and (6) can be inaccurate if two surfaces radiating to each other are too near, as it is reported, for example, in Ref. [12] or [25]. Based on intended purposes of the developed model, a direct solution of this issue is not included. However, a checking mechanism is implemented into programmed procedures, which warns if a distance between two radiating surfaces is too close and an accuracy of their radiation view factor and/or mean geometrical length could be insufficient. If a billet is placed on a ceramics hearth, than a heat flux from combustion products to a surface on the hearth or between the surface and the hearth (with regard to low temperature difference and low thermal conductivity of the hearth) is set to zero.

Emissivity of the surfaces contributing in the process and atmosphere between the surfaces are temperature dependent. The emissivity of the surfaces is therefore defined by a user database for each material and their temperature. Emissivity and/or transmissivity of the furnace atmosphere is defined by a user database for combustion products composition, their temperature and a computed mean geometric length between a solved surfaces pair. A geometrical configuration in the furnace does not change during a computation, because each beam moves to a position of a beam before it. Thus, a determination of the geometrical relations are made once only at a start of the computation.

The use of integral RVFs can be made based on the assumption of isothermal sub-zones. This assumption significantly reduces a number of solved equations compared to an element-to-element heat transfer computation used in many CFD (or FEM) numerical models. The results of a solution of the equations system (7) are the radiation heat fluxes $q_{[j]}$ into or from the individual sub-zones.

The convective heat flux in the zone is computed by the Newton relation

$$q_{k[j]}=a_{k[j]}\cdot S_{[j]}\cdot\left(tz-t_{[j]}\right) \quad (8)$$

A value of the convection coefficients $a_{k[j]}$ depends on positions of surfaces in the zone, type of burners and position of burners. The convection is mostly not as important as radiation – an estimated ratio of a convective heat transfer is about 5% at temperatures above 1000 °C. Thus, an average heat transfer coefficients for individual zones were used and local variations in some parts of the furnace, for example inlets, burners or chimney, were omitted. A general relation for heat transfer coefficient is given by a dependency of Nusselt number (Nu) on Reynolds (Re) and Prandtl (Pr) numbers $Nu = f(Re; Pr)$. The Michejev's relation $Nu = 0.032 \cdot Re^{0.8}$ was used in this work due to its simplicity. Then, a final relation for the convection coefficient can be derived in the form

$$\alpha_k=0.032\cdot\frac{\lambda_{sp}}{v_{sp}^{0.8}}\cdot\frac{w_{sp}^{0.8}}{d_h^{0.2}} \quad (9)$$

where λ_{sp}, v_{sp}, w_{sp} are thermal conductivity, kinematic viscosity and velocity of combustion products and d_h is hydraulic diameter. It is quite complicated to specify all the parameters of Eq. (9) exactly. Thus, taking into account the small influence of the convection, a convective heat transfer coefficient in a zone is defined empirically based on a configuration of burners in the zone. The values of α_k for different burners were 35 $W \cdot m^{-2} \cdot K^{-1}$ for high-speed burners, 10 $W \cdot m^{-2} \cdot K^{-1}$ for whirling burners, 5 $W \cdot m^{-2} \cdot K^{-1}$ for radiation burners and if there was not a burner in a zone. A type of burners is defined individually for upper and lower part of a zone. A heat transfer coefficient for side surfaces in the zone is determined as an average of the heat transfer coefficient of the upper and lower part.

Some parts of the beams can be shielded by a beam-moving mechanism (walking mechanism). Amount of beams bottom surface, which is shielded, is entered in percent for each zone. If the beams lie directly on a ceramic hearth (the distance is zero), the heat flux between the charge bottom surface and the hearth is assumed zero.

The geometrical model does not include any additional construction parts, which can occur in a furnace. These parts therefore does not appear in the heat transfer model, however, these parts can be assumed in the energy balance equations.

3.3. Compartment models of charge and furnace walls

Individual isothermal layers (compartments) are formed as volumes between equidistant surfaces towards the beam center, which distances are thicknesses of the layers. A geometrical representation of the 3D compartment model is shown in Fig. 2B. A temperature of each compartment is homogeneous and a conduction heat transfer is assumed between adjacent compartments. The conduction is defined by a distance of their central surfaces, by their areas, by temperature differences between the adjacent compartments and by their thermal conductivity coefficients. Each compartment (i.e. layer) represents one energy differential equation, which defines its temperature

$$\frac{dt_k}{dt}=\frac{\sum_{j=1}^{n}q_j}{m_k c_k} \quad (10)$$

where t_k is temperature of the compartment, q_i is heat flux to or from the compartment, m_k is mass of the compartment and c_k is specific

heat of the compartment. Material properties of the beams are considered temperature dependent and are updated at each time step based on an actual compartments temperature.

It is advantageous to set the first layer very thin, for example 1–2 mm for a beam cross-section dimensions ~400 mm. The temperature of this layer is also the surface temperature. Distances of other layers can be generated as a geometrical sequence based on a selected characteristic length, number of layers and a coefficient of the geometric series. Heat transfer process in furnace walls is solved in a similar way as in the beams. The walls are divided into compartments, which (unlike the beams) can be of different materials. The heat transfer is then solved as conduction between the individual compartments with temperature dependent material properties. Convection heat transfer to surface surroundings is considered at outer surface of the furnaces.

3.4. Simulation model outputs

The model solves a transient problem, so it brings results of the thermal process in every time step of the solution. The basic results of the simulation are temperature of the furnace atmosphere, temperature of the individual compartments of the furnace walls and temperature of individual compartments of the beams in all positions. However, it also makes possible to obtain heat and mass fluxes in the furnace, which brings information about heat losses in the individual furnace zones or about required power of burners.

4. Simulation inputs and temperature measurement

Experimental temperature measurement and numerical computation for the suggested model verification were performed for a gas heated continuous walking-beam furnace for steel beams reheating. The furnace length and width was 43 m and 9 m, respectively. The furnace had a capacity of 65 beams and the computational time step was 418 s. The length of a step of a movement of the beams was 660 mm and it was assumed constant along the entire furnace.

The beams had a circular cross section of diameter 410 mm and their length was 5500 mm. The beam passed through the furnace about 450 min and its maximum temperature in the soaking part of the furnace was about 1300 °C. The beams were moved by a water-cooled walking mechanism.

4.1. Thermal box-barrier temperature measurement on the furnace

Temperature of an experimental beam during its passage through the furnace was measured using a thermocouples and thermal box-barrier (TBB) in the same manner as described in Ref. [17]. A part of the measured beam was cut so that a platform was created at its end. The TBB with a temperature data logger inside was placed on the platform and the thermocouples measuring ends were installed at selected positions on the beam. The beam then moved throughout the furnace together with other beams as in a usual operation mode of the furnace. After the beam was removed from the furnace at its end, the TBB was opened and the stored temperatures in the data logger were transferred to a computer.

The temperature was measured using 7 K-type thermocouples (3 mm diameter, ceramic insulated leads with an outer Inconel coat). 6 thermocouples were located in two longitudinal positions inside the billet: at 100 mm from the end of the beam and in the center of beam; in 3 depths: its axis - 55 mm under the upper surfaces and 55 mm under the lower surface. One thermocouple was in the furnace atmosphere - about 100 mm above the top surface of the billet at its center. One thermocouple was used for a temperature monitoring in the TBB. The scheme of the placement of the thermocouples on the measured beam is shown in Fig. 3.

A declared maximum temperature usability of K-type thermocouples is 1100–1300 °C, based on a structure and a producer of the thermocouples. However, an accuracy of a thermocouple measurement decreases at temperature over about 1200 °C. This issue was partially solved by a laboratory calibration of the thermocouples. However, the most critical source of measurement errors is connected with leads of thermocouples, which are exposed to high temperature inside the furnace. An electrical-insulation layer between wires inside the thermocouples loses its properties at a high temperature. It is not a complication if a measuring end of a thermocouple is at the highest temperature. However, it can cause significant errors if the measuring end is at lower temperature than the lead of the

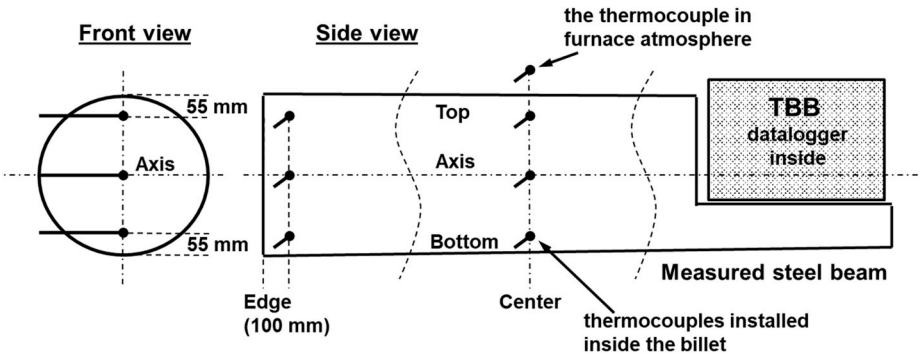

Fig. 3. Scheme of the positioning of thermocouples in the measured steel beam.

thermocouple. The error increases with an increase of a surrounding temperature (the error occurs from about 1000 °C for 3 mm diameter thermocouples and subsequently grows exponentially), of a length of the lead exposed to high temperature and of a difference between the surrounding temperature and the measured temperature at the measuring end. The error can be reduced by increasing of a diameter of the thermocouple. Thus, a number of calibration experiments was performed, including analyses of an influence of an exposure of leads of the thermocouples to high temperatures. Based on results of the experiments, thermocouples of the diameter 3 mm were selected for the measurement and the leads of thermocouples were additionally covered by high-temperature insulation mats to protect them against temperature peaks in the furnace during their passage through the furnace. Based on these steps and based on the results of the analyses performed, a measurement uncertainty at the furnace output is estimated to be about 20 °C.

4.2. Numerical model parameters

The numerical simulation inputs were in an accordance with the experimental furnace. A steady state of the furnace operation process was the required result. Thus, the total time of furnace operation simulated was 15 h. It was assumed that this time should be enough for reaching of a steady state. An initial condition for the charge and all furnace parts was 20 °C.

The furnace simulation model was divided into 11 zones. Temperature of the furnace atmosphere for each zone was defined by a temperature curve according to a technological instructions provided by the furnace operator. The required temperatures at individual zones (a heating curve) were 850, 930, 980, 930, 950, 1050, 1155, 1260, 1290, 1290 and 1275 °C. All zones were driven, that means the defined (required) temperature of the zones was controlled and maintained by burners. The defined zones temperature corresponded to temperature measured by furnace thermocouples, which were a part a heating process control system in this furnace. The definition of the temperature curve was made based on a standard production setting of the furnace and it should result to a required temperature of the heated beams at their output from the furnace.

The circular cross-section of the real beams was in accordance with above described simplifications replaced by square cross-section of dimensions 363 × 363 mm. The beams were divided into 8 compartment layers. The thickness of individual layers increased geometrically from a surface of the beam to its center. Material properties of the beams, which were made from a ferritic steel, as well as material properties of all furnace components (i.e. walls) was set in an accordance with the measured beam and real experimental furnace.

5. Results and discusion

5.1. Measurement results

Measured temperature time profiles of the furnace atmosphere and in the beam axis are shown in Fig. 4. The furnace temperature measured by a thermocouple near a top surface of the beam at its center increased up to about 700 °C immediately after the beam entered the furnace. Then it increased slowly up to about 900 °C in next 250 min of the process. A rapid temperature increase up to 1300 °C followed in next 100 min (250–350 min of the process). The furnace temperature then remained stable at the level about 1300

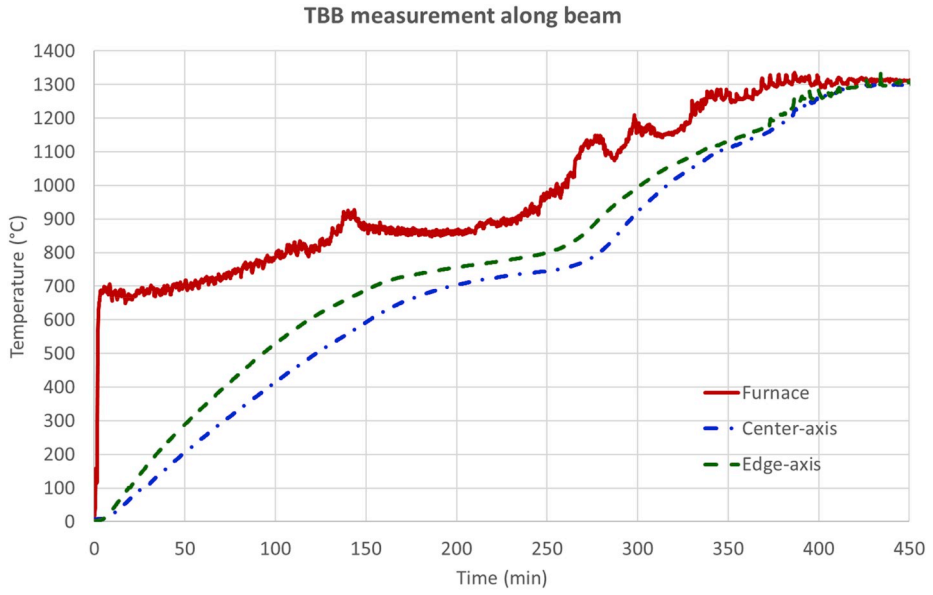

Fig. 4. Measured temperature of the beam at its center (Center-axis) and edge (Edge-axis) in its axis and measured furnace atmosphere temperature close the beam center (Furnace).

°C up to an output of the beam from the furnace. Beam temperatures followed the furnace temperature. The temperature at the beam axis at its center increased from the initial temperature (2–10 °C) to about 700 °C in 200 min (1st heating phase) and then it increased very slowly to about 750 °C in next 70 min (1st soaking phase). A second rapid increase up to temperature about 1270 °C followed from 270 to 400 min (2nd heating phase). Then, in a soaking part of the furnace (2nd soaking phase), the beam temperature was homogenized and increased slightly up to the furnace atmosphere temperature at the end of the furnace (1300 °C).

Temperature at the edges of the beam was higher than the temperature at its center by more than 100 °C during the 1st heating phase. The biggest differences were observed at heating phases. The temperature equalized in soaking phases and became homogeneous at the end of the furnace. Published results of a 3D CFD modelling, for example in Ref. [7] or [26], showed that the temperature differences decreased quickly toward a center of heated beams and might not be considered at a distance greater than approximately 1 m from the edges. However, temperature inhomogeneity along a beam length can occur due to other sources. It can occur due to beams supports, slide shoes or stepping mechanism, as it was presented for example in Ref. [2] for a pusher type furnaces with water cooled slide shoes.

As expected, the highest temperature was at the top surface of the beam and the lowest temperature was in the axis of the beam. The differences between the axis and top surface were about 50–70 °C in the 1st heating phase, then it got almost homogenized in the 1st soaking phase, the temperature differences increased again in the 2nd heating phase up to about 100 °C and, finally, the temperature homogenized at the 2nd soaking phase. The differences of the temperature between the top surface, the bottom surface and the axis of the beam were not so high in course of a passage of the beam throughout the furnace. This is an important information from the point of view of unwanted deformations of the beams.

The temperature time profile measured by the thermocouple in the furnace was scattered and there was a number of local fluctuations. These fluctuations were mostly caused by local temperature changes due to a variable flow of combustion products and geometrical arrangement of an interior of the furnace (position of burners, temperature regulation by switching burners on/off etc.). The used thermocouple was relatively thin and, therefore, sensitive to these local short-term temperature changes. On the other hand, the time-temperature curves measured by thermocouples inside the beam were smooth because of a mass of the steel beam.

5.2. *Numerical model results and verification*

A comparison of modelled and measured temperatures is shown in Fig. 5. The measured temperatures were obtained at the center of the beam. The modelled temperatures were taken from the 5th compartment layer, which position corresponded to the placement of the thermocouples. The simulated temperature courses followed a shape of the measured time-temperature curves. However, the simulated temperatures were notably higher than the measured values. This disagreement was most significant in the 1st heating phase (0–150 min), where the differences were up to about 100–200 °C.

The discrepancy between modelled and measured temperature showed a very important fact regarding the zonal model approach. Two connected reasons of this disagreement were found. The first reason is connected with a temperature averaging in the zones. The zonal model is based on an assumption of an average temperature in a zone. The zones temperatures were defined by a temperature curve based on a required heating of the beams. The zones temperatures are determined by furnace thermocouples, which were used for a control of a furnace operation. A desired temperature of the first zone of the furnace was 850 °C and the simulated temperature at

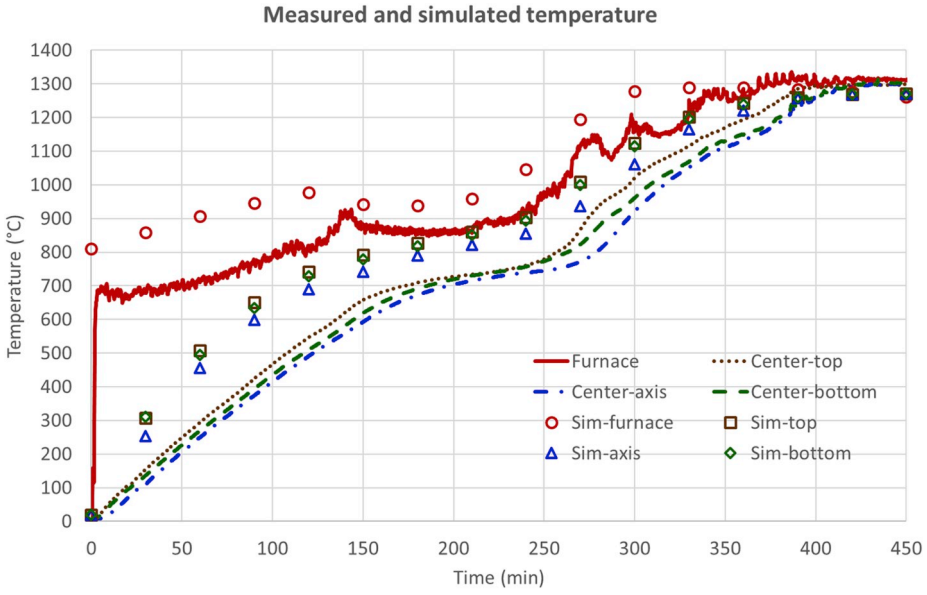

Fig. 5. Comparison of measured (lines) and simulated (points) temperature of the furnace atmosphere (Furnace) and of the beam in its axis (-axis), at its top surface (-top), at its bottom surface (-bottom).

the start of the furnace was about 810 °C.

The second reason is connected with a method of a measurement of the temperature in the zones. The thermocouples were heated by both convection and radiation processes. The measured values were therefore a combination of a combustion products temperature at a position of the thermocouples and a radiative heating from sources around the thermocouples (furnace atmosphere, beams, walls etc.). The experimental thermocouple in the furnace atmosphere was thinner and thus more sensitive for local temperature fluctuations. The furnace thermocouples were in a ceramics casing which made them more stable and less sensitive to short-term furnace temperature fluctuations. A material and optical properties of the casings were also different. The most significant differences were however in a placement of the thermocouples. The experimental one was near the measured beam and it moved together with the beam along the furnace. The furnace thermocouples were near a roof of the furnace. All these facts caused differences in measured temperatures between the experimental thermocouple and the furnace thermocouples.

The comparison of the experimental and numerical results implied that the data obtained near the investigated beam were more relevant for a definition of the heating curve. Thus, a new temperature curve of the furnace atmosphere was defined for the numerical simulation based on the experimental results. The modified required temperatures at individual zones were 710, 790, 855, 870, 895, 970, 1070, 1160, 1250, 1325 and 1350 °C. Numerical simulation results obtained using the modified heating curve together with the measured temperatures are in Fig. 6.

The furnace atmosphere temperatures obtained by the experiment and numerical simulation were in a better accordance after the modification of the heating curve. The simulated beam temperatures were still higher than the measured of about 100 °C in the 1st heating phase. However, the simulated and measured results came together in the 1st soaking phase and were very similar in the rest of the heating process. Especially the temperatures in the beam axis were in a very good agreement – the differences between measured and simulated temperatures were from 10 to 20 °C. These results were considered satisfactory with respect to an expected measurement accuracy and simplifications of the used numerical model approach.

The numerical model presented in this work is not intended for solving of processes related to any local temperature differences. Thus, it is not able to compute differences between an axis of the beam and edges of the beam. However, the model used a dividing of the beam geometrical model to an upper, bottom and side zones, which were composed of individual isothermal layers/compartments. The model made therefore possible to solve temperature differences between upper and bottom surfaces of the beams. The numerical computation results showed, in accordance with the experiment, that the lowest temperature was in the beam axis. A temperature difference between the axis and top surface was about 100 °C. It partly equalized in the 1st soaking phase and the differences increased again in the 2nd heating phase. Differences between the axis and top/bottom surface temperatures decreased to about 10 °C in the 2nd soaking phase.

6. Conclusions

A numerical simulation model was introduced, which was developed for a simulation of a steel beams heating procedure in a continuous walking-beam furnace. The model was transient and it was based on a dividing of the furnace to isothermal zones and dividing of the charge and furnace parts into isothermal compartment layers. It was shown that it was possible to make a computation of a heating process leading to a steady state solution. The model allowed determination of beams temperature at different positions in

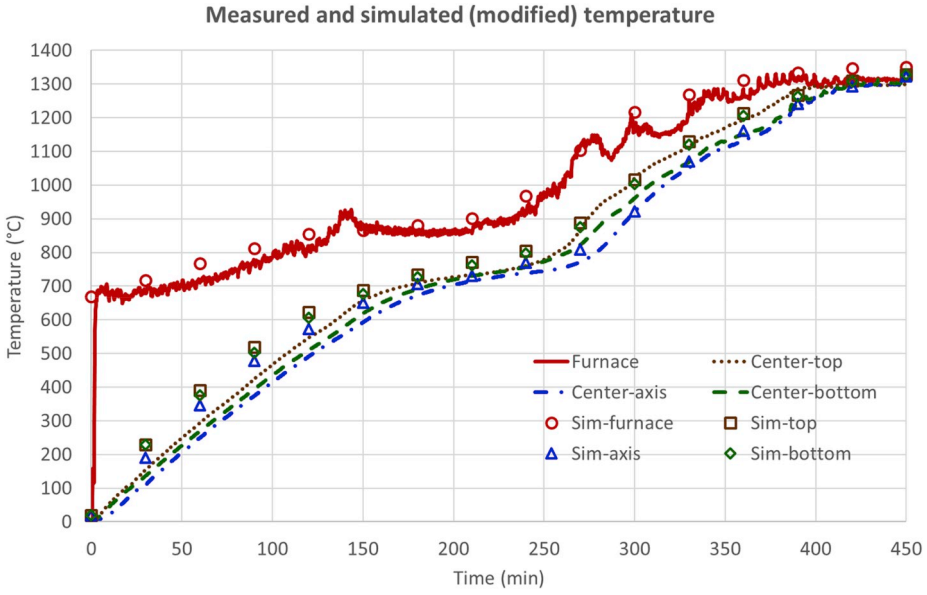

Fig. 6. Simulation results with the modified heating curve. Comparison of measured (lines) and simulated (points) temperature of the furnace atmosphere (Furnace) and of the beam in its axis (-axis), at its top surface (-top), at its bottom surface (-bottom).

the furnace. Despite used simplifications, the model included definitions of all important parameters regarding the furnace, beams and heating process. Even if some knowledge regarding furnace operation generally was necessary, the results showed that the model was a general enough tool for an analysis of a heating procedure in a walking-beam furnace.

An experiment of a tested beam temperature measurement was performed. The measurement procedure using a thermal box-barrier made possible a continuous temperature measurement of the tested beam and of a furnace atmosphere near the beam during its passage throughout the furnace. This measurement therefore appeared as a suitable tool for a verification of the numerical model.

A comparison of simulated and measured temperatures of the tested beam showed a discrepancy between measured and simulated data if a heating curve was specified based on furnace thermocouples, which were used for a control of an operation of the furnace. The differences about 200 °C between the simulated and measured temperature profiles were caused by temperature averaging made by the zonal model and different locations of the thermocouples in the furnace – the experimental thermocouple was near the tested beam while the furnace thermocouples were near a roof of the furnace. It was demonstrated that the temperatures obtained near the tested beam were in this case more relevant for a definition of required temperature in individual zones of the zonal model than the furnace thermocouples data provided by a furnace operator.

A very good agreement was achieved between the experiment and simulation after a modification of the heating curve was made in accordance to the temperature measured during the experiment. The differences between the measured and experimental beam temperatures were about 100 °C at the start of the heating process and from 10 to 20 °C at the end of the furnace. The simulation and the experiment were also in a good agreement in relation to a temperature distribution in a beam cross section. It was shown that the differences between the beam axis and top/bottom surfaces temperatures were about 100 °C at the start of the heating process. The temperature of the beam equalized during its passage through the furnace and the temperature differences were about 10 °C at the furnace output.

The used approach allowed to perform the computation using a standard personal computer (2.40 GHz, 8 GB RAM) in about 25 min. This result is significantly better than full-featured CFD models (e.g. 34 h reported in Ref. [6]). The CFD models based on finite volumes or finite elements discretization are of course more general and allow more exact implementation of physical processes in a furnace. On the other hand, the simulation time is too long for on-line control simulation models, where a real-time computing is mostly required. However, simulation models for an on-line control should often be significantly simplified to achieve a sufficient computation speed. That is demonstrated for example in Ref. [9], where a 1D model with inputs obtained by calibration measurement of a specific furnace is used. Thus, the approach presented in this contribution could be a good compromise between a versatility allowing flexible changes of process parameters, computation time allowing repeated calculations and accuracy, which was verified by the measurement. The suggested approach could be, for example, a good tool for an initial furnace parameters design or for a design of a heating process for different charge characteristics or processing requirements.

Declaration of competing interest

The corresponding author declares on behalf of all authors that they has no conflict of interest.

CRediT authorship contribution statement

Michal Švantner: Conceptualization, Methodology, Validation, Investigation, Resources, Writing - original draft, Writing - review & editing, Supervision. **Josef Študent:** Conceptualization, Methodology, Software, Validation, Formal analysis, Resources, Writing - original draft. **Zdeněk Veselý:** Resources, Writing - original draft, Writing - review & editing.

Acknowledgement

The work was supported by ERDF project “LABIR-PAV/Pre-application research of infrared technologies” Reg. No. CZ.02.1.01/0.0/0.0/18_069/0010018.

References

[1] W. Trinks, M.H. Mawhinney, R.H. Shannon, R.J. Reed, J.R. Garvey, Industrial Furnaces, sixth ed., John Wiley & Sons, New Jersey, 2004.
[2] M. Honner, Z. Vesely, M. Svantner, Temperature and heat transfer measurement in continuous reheating furnaces, Scand. J. Metall. 32 (2003) 225–232, https://doi.org/10.1034/j.1600-0692.2003.00645.x.
[3] A.A. Minea, Advances in Industrial Heat Transfer, CRC Press - Taylor & Francis Group, Boca Raton, 2012.
[4] E. Hachem, G. Jannoun, J. Veysset, M. Henri, R. Pierrot, I. Poitrault, E. Massoni, T. Coupez, Modeling of heat transfer and turbulent flows inside industrial furnaces, Simulat. Model. Pract. Theor. 30 (2013) 35–53, https://doi.org/10.1016/j.simpat.2012.07.013.
[5] C.-T. Hsieh, M.-J. Huang, S.-T. Lee, C.-H. Wang, Numerical modeling of a walking-beam-type slab reheating furnace, Numer. Heat Tran. A Appl. 53 (2008) 966–981, https://doi.org/10.1080/10407780701789831.
[6] S.H. Han, D. Chang, Optimum residence time analysis for a walking beam type reheating furnace, Int. J. Heat Mass Tran. 55 (2012) 4079–4087, https://doi.org/10.1016/j.ijheatmasstransfer.2012.03.049.
[7] J.M. Casal, J. Porteiro, J.L. Míguez, A. Vázquez, New methodology for CFD three-dimensional simulation of a walking beam type reheating furnace in steady state, Appl. Therm. Eng. 86 (2015) 69–80, https://doi.org/10.1016/j.applthermaleng.2015.04.020.
[8] V.K. Singh, P. Talukdar, P.J. Coelho, Performance evaluation of two heat transfer models of a walking beam type reheat furnace, Heat Tran. Eng. 36 (2015) 91–101, https://doi.org/10.1080/01457632.2014.906287.

[9] M. Honner, Z. Vesely, M. Svantner, Exodus stochastic method application in the continuous reheating furnace control system, Scand. J. Metall. 33 (2004) 328–337, https://doi.org/10.1111/j.1600-0692.2004.00703.x.
[10] M. Landfahrer, C. Schluckner, R. Prieler, H. Gerhardter, T. Zmek, J. Klarner, C. Hochenauer, Development and application of a numerically efficient model describing a rotary hearth furnace using CFD, Energy 180 (2019) 79–89, https://doi.org/10.1016/j.energy.2019.04.091.
[11] A. Emadi, A. Saboonchi, M. Taheri, S. Hassanpour, Heating characteristics of billet in a walking hearth type reheating furnace, Appl. Therm. Eng. 63 (2014) 396–405, https://doi.org/10.1016/j.applthermaleng.2013.11.003.
[12] H. Ebrahimi, A. Zamaniyan, J.S. Soltan Mohammadzadeh, A.A. Khalili, Zonal modeling of radiative heat transfer in industrial furnaces using simplified model for exchange area calculation, Appl. Math. Model. 37 (2013) 8004–8015, https://doi.org/10.1016/j.apm.2013.02.053.
[13] R. Méchi, H. F, R. Saïd, Improved zonal method predictions in a rectangular furnace by smoothing the exchange areas, Turk. J. Eng. Environ. Sci. 31 (2007) 333–343, https://doi.org/10.3906/TAR-1206-53.
[14] E. McGee, P.A. Roach, C.-K. Tan, A. Matthew, Y. Hu, J. Broughton, Development of transient mathematical models for a large-scale reheating furnace using hybrid zone-CFD methods, Energy Procedia 75 (2015) 3076–3082, https://doi.org/10.1016/j.egypro.2015.07.633.
[15] M. Švantner, P. Vacíková, M. Honner, Non-contact charge temperature measurement on industrial continuous furnaces and steel charge emissivity analysis, Infrared Phys. Technol. 61 (2013) 20–26, https://doi.org/10.1016/j.infrared.2013.07.005.
[16] M. Landfahrer, R. Prieler, B. Mayr, H. Gerhardter, T. Zmek, J. Klarner, C. Hochenauer, Characterization of the temperature distribution on steel tubes for different operating conditions in a reheating furnace using CFD and three different measuring methods, Appl. Therm. Eng. 133 (2018) 39–48, https://doi.org/10.1016/j.applthermaleng.2017.12.098.
[17] M. Honner, M. Švantner, Thermal box-barrier for a direct measurement in high temperature environment, Appl. Therm. Eng. 27 (2007) 560–567, https://doi.org/10.1016/j.applthermaleng.2006.06.004.
[18] J. Martinec, H. Šen, K. Svoboda, J.V. Martincová, D. Baxter, The thermal protection of a specific experimental instrument for monitoring of combustion conditions on the grate of municipal solid waste incinerators, Appl. Therm. Eng. 30 (2010) 1022–1028, https://doi.org/10.1016/j.applthermaleng.2010.01.014.
[19] M.Y. Kim, A heat transfer model for the analysis of transient heating of the slab in a direct-fired walking beam type reheating furnace, Int. J. Heat Mass Tran. 50 (2007) 3740–3748, https://doi.org/10.1016/j.ijheatmasstransfer.2007.02.023.
[20] S.H. Han, S.W. Baek, M.Y. Kim, Transient radiative heating characteristics of slabs in a walking beam type reheating furnace, Int. J. Heat Mass Tran. 52 (2009) 1005–1011, https://doi.org/10.1016/j.ijheatmasstransfer.2008.07.030.
[21] A. Jaklič, T. Kolenko, B. Zupančič, The influence of the space between the billets on the productivity of a continuous walking-beam furnace, Appl. Therm. Eng. 25 (2005) 783–795, https://doi.org/10.1016/j.applthermaleng.2004.07.012.
[22] M.F. Modest, Radiative Heat Transfer, third ed., Academic Press, Oxford, 2013.
[23] H.C. Hottel, A.F. Sarofim, Radiative Transfer, McGraw-Hill, 1967.
[24] H.C. Hottel, E.S. Cohen, Radiant heat exchange in a gas-filled enclosure: allowance for nonuniformity of gas temperature, AIChE J. 4 (1958) 3–14, https://doi.org/10.1002/aic.690040103.
[25] M.P. Mengüç, R. Viskanta, Radiative transfer in three-dimensional rectangular enclosures containing inhomogeneous, anisotropically scattering media, J. Quant. Spectrosc. Radiat. Transf. 33 (1985) 533–549, https://doi.org/10.1016/0022-4073(85)90021-4.
[26] M. Gu, G. Chen, X. Liu, C. Wu, H. Chu, Numerical simulation of slab heating process in a regenerative walking beam reheating furnace, Int. J. Heat Mass Tran. 76 (2014) 405–410, https://doi.org/10.1016/j.ijheatmasstransfer.2014.04.061.